HHS Public Access

Author manuscript

Biochim Biophys Acta. Author manuscript; available in PMC 2018 February 01.

Published in final edited form as:

Biochim Biophys Acta. 2017 February ; 1861(2): 441–449. doi:10.1016/j.bbagen.2016.10.008.

Photobiomodulation of human adipose-derived stem cells using 810nm and 980nm lasers operates via different mechanisms of action

Yuguang Wang[1,2,3,4], **Ying-Ying Huang**[3,4], **Yong Wang**[1,2], **Peijun Lyu**[1,2,*], and **Michael R Hamblin**[3,4,5,*]

[1]Center of Digital Dentistry, Peking University School and Hospital of Stomatology, Beijing China

[2]National Engineering Laboratory for Digital and Material Technology of Stomatology, Beijing, China

[3]Wellman Center for Photomedicine, Massachusetts General Hospital, Boston, MA, 02114, USA

[4]Department of Dermatology, Harvard Medical School, Boston, MA, 02115, USA

[5]Harvard-MIT Division of Health Sciences and Technology, Cambridge, MA, 02139, USA

Abstract

Photobiomodulation (PBM) using red or near-infrared (NIR) light has been used to stimulate the proliferation and differentiation of adipose-derived stem cells. The use of NIR wavelengths such as 810nm is reasonably well accepted to stimulate mitochondrial activity and ATP production via absorption of photons by cytochrome c oxidase. However, the mechanism of action of 980nm is less well understood. Here we study the effects of both wavelengths (810 nm and 980 nm) on adipose-derived stem cells in vitro. Both wavelengths showed a biphasic dose response, but 810nm had a peak dose response at 3J/cm^2 for stimulation of proliferation at 24 hours, while the peak dose for 980nm was 10–100 times lower at 0.03 or 0.3 J/cm^2. Moreover, 980nm (but not 810nm) increased cytosolic calcium while decreasing mitochondrial calcium. The effects of 980nm could be blocked by calcium channel blockers (capsazepine for TRPV1 and SKF96365 for TRPC channels), which had no effect on 810nm. To test the hypothesis that the chromophore for 980nm was intracellular water, which could possibly form a microscopic temperature gradient upon laser irradiation, we added cold medium (4°C) during the light exposure, or pre-incubated the cells at 42°C, both of which abrogated the effect of 980nm but not 810nm. We conclude that 980nm affects temperature-gated calcium ion channels, while 810nm largely affects mitochondrial cytochrome c oxidase.

Graphical abstract

[*]Corresponding authors: Peijun Lyu: Tel. +86 10 62188981; fax. +86 10 62142111. kqlpj@bjmu.edu.cn; Michael R Hamblin: Tel. +1 617-726-6182; fax. 617-726-8566. hamblin@helix.mgh.harvard.edu.

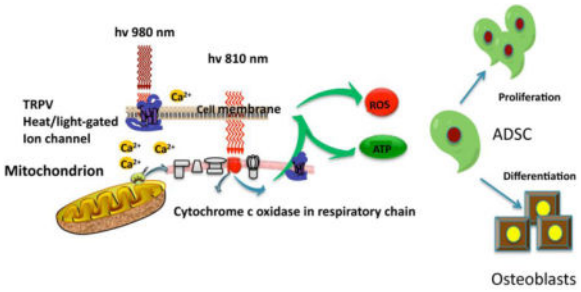

Keywords

photobiomodulation; adipose-derived stem cells; 810 nm; 980 nm; cytochrome c oxidase; heat-gated ion channels

Introduction

Photobiomodulation (PBM) uses visible red or near-infrared (NIR) light to produce a range of beneficial therapeutic effects, which can be used to treat many different diseases and disorders [1]. PBM (therapy) has recently been introduced as the recommended index term to replace the technique that was previously known as “low level laser (light) therapy” [2].

There have been many different molecules that have been proposed over the years to act as the primary photoacceptor or chromophore in PBM [3]. The first law of photobiology states that a photon must be absorbed by a specific chromophore located inside cells or tissues to have any biological effect. The primary chromophore which has been most often discussed in PBM is cytochrome c oxidase (CCO), which comprises unit IV in the mitochondrial respiratory chain [4]. CCO has two absorption bands, one in the red spectral region (~660 nm) and another in the NIR spectrum (~800 nm), which happen to match the wavelengths most often used in PBM. One popular theory is that nitric oxide (which acts as a competitive inhibitor of oxygen binding) can be photo-dissociated from its binding sites (copper and heme centers in CCO), after which electron transport, mitochondrial metabolism and ATP production will rapidly increase [5]. However the absorption bands of CCO become much weaker at wavelengths greater than 900 nm, which suggests that alternative chromophores must exist, in order to absorb long wavelength photons between 900 nm in the NIR region and all the way out to 20 μm in the far-infrared spectrum [6]. The identity of this long wavelength chromophore is still uncertain, but water is the obvious candidate based on its absorption spectrum in the IR spectrum, and its high abundance in biological systems. Moreover, shorter wavelengths in the blue and green spectral regions may be absorbed by yet other, different chromophores in cells such as (for instance) flavins [7].

Among many uses of PBM in cell culture, stimulation of the proliferation and differentiation of adipose derived stem cells (ADSC) or other kinds of mesenchymnal stem cells, has been frequently investigated [8–13]. Many workers have studied the ability of PBM to encourage ADSC to differentiate down the osteogenic pathway and become osteoblasts [14–16].

The present study was designed to compare the mechanisms of action of two different NIR wavelengths (810 nm and 980 nm) on the proliferation and differentiation of ADSC. We tested the hypothesis that 980 nm has a different chromophore, and therefore a different mechanism of action, from those commonly attributed to 810 nm.

Material and Methods

Cell culture

hASCS were purchased from ScienCell Company (San Diego, CA, USA). Cells in the fourth passage were used for the proliferation and differentiation experiments. All experiments were repeated at least three times. All materials were purchased from Sigma-Aldrich (St. Louis, MO) unless stated otherwise. Cells were routinely cultured in proliferation medium (PM) which contains Dulbecco's modified Eagle medium (DMEM, Gibco BRL, Grand Island, NJ) containing 10% fetal bovine serum (Atlanta Biologicals, Flowery Branch, GA), 100 IU/ml penicillin/streptomycin. Osteogenic differentiation medium (OM) for hASCs was composed of high glucose Dulbecco's modified Eagle medium (DMEM) containing 10% fetal bovine serum, 100 IU/ml penicillin/streptomycin, 100 nM dexamethasone, 0.2 mM ascorbic acid, and 10 mM β-glycerophosphate.

Cell proliferation assay

In cell proliferation assays, cells were cultured in PM with various fluences of photobiomodulation. Cell number was determined by using the Sulforhodamine B colorimetric assay (SRB) according to the recommended protocol [17]. SRB measures the amount of cellular protein and does not rely on mitochondrial activity. Growth curves were constructed using the OD values of the SRB assay (mean ±SD, n=8)

Osteogenic cell differentiation protocol

Cells were seeded in 6-well plates at a density of $2*10^4/cm^2$ and cultured in OM with or without photobiomodulation. Alkaline phosphatase (ALP) activity was measured on the 7th day of osteoinduction using an ALP kit (#SCR004, Millipore) according to the manufacturer's protocol.

To determine the degree of mineralization produced by differentiation, Alizarin red S (AR-S) staining was used after 21 days of culture. To quantify matrix mineralization, AR-S-stained samples were treated with 100mM cetylpyridinium chloride for 60 min to solubilize the calcium-bound AR-S into the solution. The absorbance was measured at 562nm to determine the quantity of the released calcium-bound AR-S.

Photobiomodulation, pharmacological compounds, cold and heat treatment

The cells were irradiated using two different wavelengths of PBM (810nm and 980 nm), and for each wavelength a range of different doses (0.03 to 10 J/cm^2) were used to find the best parameters for cell proliferation in each case. For the osteogenic differentiation assay, $3J/cm^2$ was used for 810nm, and 0.3J cm^2 for 980nm on the first day in OM, and the light was repeated five times every two days for 10 days in total. During this process, RUNX2 was only detected on day 7 (after 3 applications of PBM) and at 14 days (after 5 applications

of PBM). Alizarin Red staining assay was carried out at 21 days, and all the other assays were measured after 14 days. The different light sources are listed in Table 1. The chemicals were added into the culture medium 10 min before photobiomodulation, and at the end of light exposure were washed out with PBS.

Capsazepine (CPZ) is a selective inhibitor of transient receptor potential vanilloid 1 (TRPV1) ion channel, and SKF96365 (SKF) is a non-selective inhibitor of transient receptor potential canonical (TRPC) ion channels. Calphostin C (CC) is a selective inhibitor of protein kinase C (PKC). CPZ, SKF and CC were dissolved in DMSO at a concentration of 10mM and a final concentration of 5μM (2000 fold dilution) for CPZ and SKF, 100nM (100,000 fold dilution) for CC were used for the experiments.

In some experiments the cells were subjected to cold or heat treatment. For cold treatment, the cells were kept in 4°C medium only during the time period needed to deliver the PBM (out of the incubator); immediately after irradiation the hASCs were changed back to 37 °C medium and returned to the incubator. For heat treatment, cells were pre-incubated for 1 hour in the 42 °C incubator, and then immediately received laser irradiation, and were returned to the 37°C incubator.

RNA Extraction, Reverse Transcription, and Quantitative RT-PCR

In order to compare the effects of these two wavelengths of PBM, and to study the effects on TRP channels and PKC inhibitors on osteogenic markers, quantitative PCR was performed.

Total cellular RNA was isolated with RNeasy Mini Kit (QIAGEN, Valencia, CA) and reverse transcribed using High-Capacity RNA-to-cDNA™ Kit System (Applied Biosystems, Foster City, CA). Quantification of all gene transcripts was performed by real-time polymerase chain reaction (RT-PCR) using a SYBR Green kit (Roche Diagnostics Ltd, Lewes, UK). GAPDH was used as an internal control. The primers used are listed in Table 2.

Intracellular calcium assay

To monitor changes in the intracellular calcium in hASCs, cells were pretreated with 1μM Fluo-4 AM for 1 hour before photobiomodulation. Then 810nm or 980nm wavelength light was applied and confocal imaging or flow cytometry were carried out immediately.

ATP production assay

To measure the ATP generation, CellTiter-Glo Luminescent Cell Viability Assay (Promega, Madision, WI) was used to determine the ATP level after photobiomodulation. According to the protocol of the manufacturer, luminescence was recorded with a SpectraMax M5 Multi-Mode Microplate Reader (Molecular Devices, Sunnyvale, CA, USA). The experiment was repeated 3 times (mean ± SD, n=8).

Mitochondrial membrane potential determination

Mitochondrial membrane potential (MMP) was monitored with tetramethylrhodamine methyl ester (TMRM). TMRM was added to hASCs at a concentration of 25nM at 37°C for 15 min. Cells were then washed with PBS. Live Cell Imaging Solution (LCIS, Invitrogen,

Darmstadt, Germany) with 10% FBS was used to maintain cell viability in longer time courses. Cells were analyzed by confocal microscopy or by flow cytometry.

Evaluation of cellular ROS production

To evaluate the production of intracellular ROS, a fluorescent indicator CM-H2DCFDA (general oxidative stress indicator) was used after PBM. After incubating with 5μM of CM-H2DCFDA for 15min, cells were washed with PBS. The fluorescence was measured by confocal microscope or flow cytometry.

Statistical Analysis

All assays were performed in triplicate with n=6 for each sample repetition. Graphpad Prism 6.0 was used to perform Single-Factor ANOVA with a Tukey's post-hoc test to evaluate the statistical significance of experimental results ($P < 0.05$). For multiple comparisons, Bonferroni was used in all the experiments. The 2ˆdelta delta Ct method was used in relative gene expression studies.

Result

1. Compared with 810nm, 980nm produces better effects on hASC proliferation at a lower fluence

We found that both wavelengths showed a biphasic dose response, lower doses of both wavelengths showed stimulation, but high doses (20J/cm^2) of 810nm and 980nm irradiation, produced biological inhibition (Figure 1A). However 810nm exhibited a peak dose response at 3J/cm^2 for proliferation at 24 hours, while 980nm showed better effects on cell proliferation at much lower doses (10–100 times lower at 0.03 or 0.3 J/cm^2). Figure 1A shows that 0.3 J/cm^2 of 980nm laser (proliferation 40% above control) had the best effects on cell proliferation ($P<0.001$) compared with other doses of 980nm, and the 810nm groups. While the ATP level showed the same overall trend (Figure 1B), the dose of 0.3 J/cm^2 of 980nm had better effects than the other groups.

In both the ATP and SRB experiments, the lasers all showed the phenomenon of bi-directional regulation. With the increase of the laser dosage, the biological promoting effect was weakened and the biological inhibition was changed.

2. Effects of 980 nm compared with 810 nm on mitochondrial membrane potential (MMP), intracellular calcium, time course of intracellular ROS; effects of irradiance and fluence of 980 nm on MMP and ROS

In the following set of experiments, we compared the effects of two doses of 810 nm and 980 nm (0.3J/cm^2 and 3J/cm^2) delivered at 50mW/cm^2 on MMP (Fig 2A), intracellular calcium (Fig 2B), and time course of ROS production (Fig 2C). We then compared the effects of two different power densities (15mW/cm^2 and 75mW/cm^2), and different doses of 980 nm on MMP (Fig 2D) and on ROS (Fig 2E)

Figure 2A shows that 0.3J/cm^2 of 810 nm had no significant effect on MMP, while the same dose (0.3J/cm^2) of 980 nm had the largest effect (15% increase). By contrast when the doses

were increased to 3J/cm^2 the effects of both wavelengths were similar (about 10% increase) and were significantly different from both control and 0.3J/cm^2 of 980nm. In Figure 2B the effects on intracellular calcium can be seen. Only 0.3J/cm^2 of 980 produced a large significant increase while the other three parameters only produced small non-significant increases. Figure 2C shows the effects of what appeared to be the most effective sets of parameters (3J/cm^2 of 810 nm and 0.3J/cm^2 of 980 nm) on intracellular ROS production. As both conditions appeared to produce ROS in preliminary experiments we carried out a time course over 6 hours. In can be seen that while both conditions produced a similar peak in ROS, the peak occurred faster at 10–20 min with 0.3J/cm^2 of 980 nm, while the peak was later at 40 min with 3J/cm^2 of 810 nm.

We also found a biphasic response of 980 nm with irradiance (comparing 15mW/cm^2 and 75mW/cm^2) and with fluence (comparing 0.3J/cm^2 and 3J/cm^2). Figure 2D shows that for MMP the low fluence delivered at the low irradiance produced the biggest increase, while the high fluence delivered at the low irradiance also produced an increase. By contrast, both fluences delivered at the high irradiance produced a decrease in MMP, and this was significant at 0.3J/cm^2. When these comparisons were repeated with intracellular ROS as shown in Figure 2E, an effect of both irradiance and fluence was seen. The low fluence at the high irradiance produced the biggest increase, while the low fluence at the low irradiance also produced a significant increase.

3. The ability of 980 nm (but not 810nm) to promote cell proliferation could be abrogated by TRPV1/TRPC channel inhibitors, and also by cold treatment

To further explore whether 0.3 J/cm^2 of 980 nm and 3 J/cm^2 of 810 nm promoted cell proliferation though the same signaling pathway, we tested the hypothesis that heat-activated ion channels could be involved. SKF (TRPC channel inhibitor), CPZ (TRPV1 channel inhibitor) and cold treatment (TRPV1 is also a heat gated ion channel) were used. hASCs were pretreated with 10μM of SKF and CPZ 10min before PBM. For cold treatment, the cells were kept in 4°C medium during the time period needed for PBM, immediately after irradiation the hASCs were changed back to 37 °C medium and returned to the incubator immediately. Capsaicin, a TRPV1 agonist, which has been reported to activate TRPV1, and thereby promote cell proliferation and increase ATP production at a concentration of 1μM, was used as a positive control. As expected from the literature, the effects of capsaicin could be abrogated by the TRPV1 inhibitor CPZ (Figs 3A and 3B). hASCs were incubated with CPZ for 10 min, then washed with PBS 3 times and then returned to PM. We found that CPZ, SKF and cold treatment did not affect cell proliferation (Fig 3A) or ATP production (Fig 3B). The proliferation promoting effects of 980 nm could be abrogated by SKF, CPZ and by cold treatment, but there was no significant difference between the effect of 810nm alone and any of the inhibitory treatments (SKF CPZ, cold treatment) (Fig 3A). We found very similar effects of these three inhibitory treatments on the increase in ATP produced by 0.3 J/cm^2 of 980 nm (all three treatments were effective) and by 3 J/cm^2 of 810 nm (none of the three treatments were effective) (Fig 3B).

In order to further elucidate whether 980 nm could promote cell proliferation via a TRPV1 calcium ion channel pathway, we used Fluo-4 to measure the intracellular calcium and

Rhod-2 to measure the mitochondrial calcium. We found that the intracellular calcium showed a sharp increase 30s after PBM. The peak in the 0.3J/cm^2 980nm group was higher than the 3J/cm^2 980nm group, and the calcium peak in the 0.3J/cm^2 980nm could be inhibited by SKF, CPZ and cold treatment (Figs 3C and 3D). For mitochondrial calcium (Fig 3E), there was a sharp decrease with both 0.3/cm^2 and 3J/cm^2 980nm groups, and the decrease of mitochondrial calcium in the 0.3/cm^2 980nm group could be abrogated by SKF, CPZ and cold treatment (Fig 3E). There was no significant differences in calcium between 810 nm group and 810 nm + SKF, CPZ, or Cold treatment groups (Data not shown).

4. Heat treatment and the combined effects of heat and PBM on cell proliferation

Studies have shown that incubating cells in 42°C medium could activate heat gated ion channel TRPV1 [18], and mild hyperthermia could promote cell proliferation in hASC and other stem cells [19, 20]. To further explore whether PBM using 980nm could promote cell proliferation via activation of the heat gated ion channel, TRPV1 we incubated hASCs for one hour in a 42°C incubator, then moved the cells back to the 37°C incubator. We found that one hour of incubation at 42°C could enhance cell proliferation and increase the production of ATP, and that these processes could be blocked by TRPV1 channel inhibitors (CPZ and SKF). If the cells were pre-incubated for 1 hour in the 42 °C incubator, and then received laser irradiation, we found that cell proliferation in the 0.3 J/cm^2 980nm group was significantly better than the 980nm + 42°C group, while the 3J/cm^2 810nm + 42°C group was better than the 810nm alone group. These results show that the stimulatory effects of 980nm laser on hASC proliferation can be inhibited by mild heat at 42°C, therefore the mechanisms of 980 nm and 42 °C hyperthermia may have a common pathway. However the effects of 42°C on the stimulation of proliferation by 810nm laser were additive rather than inhibited, and therefore 810 nm and 42 °C hyperthermia probably do not share a common pathway.

5. The ability of 980nm, but not 810nm to promote osteogenic cell differentiation could be abrogated by TRPV1 and TRPC channel inhibitors

To further explore if the pathways by which 0.3 J/cm^2 of 980 PBM nm and 3 J/cm^2 of 810 nm PBM can promote hASC differentiation down the osteogenic pathway are different, the ion channel inhibitors, SKF and CPZ were used to block calcium ion channels. hASCs were pretreated with 10μM of SKF and CPZ 10min before each of five applications of PBM over a 14 day period. Alizarin Red staining carried out after 21 days showed that the differentiation promoting effects of 980 nm PBM could be abrogated by SKF and CPZ, but there was no significant difference between 810 nm and the 810 nm + CPZ or SKF groups (Figs 5A, 5B and 5C). We found that both 3 J/cm^2 of 810nm PBM and 0.3 J/cm^2 of 980nm PBM could upregulate osteogenic-related gene expression, and the 980nm laser achieved better effects than 810nm (Fig 5D). When comparing 810nm alone, and 810nm + CPZ or SKF groups, there was no significant difference in osteogenic-related gene expression. In contrast, there was no up-regulation osteogenesis-related genes in 980nm + CPZ or SKF groups (Fig 5D).

Discussion

The present study has found interesting and remarkable differences in the mechanisms of action of the PBM effects using two different NIR wavelengths. The pronounced biphasic dose response found with both of these wavelengths necessitated the use of a different fluence of each wavelength (0.3 J/cm^2 of 980 nm and 3 J/cm^2 of 810 nm) in order to achieve the optimum stimulation of the various readouts that were employed in the different assays.

Wavelengths in the region of 810 nm (780 nm, 800 nm, 830 nm, 850 nm, 880 nm, etc) have been one of the most popular ranges of wavelengths used for PBM applications with hundreds of published studies. It is reasonably well established that photons with these NIR wavelengths are absorbed by chromophores in CCO, and stimulate mitochondrial metabolism (shown by raised MMP and more oxygen consumption) and therefore increase ATP production. The most often cited molecular mechanism for this stimulation of CCO activity, is the photodissociation of inhibitory nitric oxide that binds to the heme or copper centers in the enzyme, that prevents oxygen from reaching the active site, and thus limiting respiration and ATP production [18].

On the other hand, although wavelengths around 980 nm have been less frequently used for PBM, there have indeed been some reports of these wavelengths being employed in a diverse range of pathologies including wound healing in vitro [21], oral lichen planus in humans [22], an adjunct to non-surgical periodontal treatment in humans [23], control of pain, swelling, and trismus associated with surgical removal of impacted lower third molars in humans [24]. Moreover Anders et al showed 980 nm light could increase the rate of nerve regeneration in a rabbit model [25]. In medical applications, 980 nm lasers were originally developed to target the water absorption peak centered at 975 nm. High power focused 980 nm lasers have been used for tissue coagulation [26] and tissue ablation [27]. This photothermal targeting of water, combined with the relative lack of absorption peaks due to CCO at this wavelength (980 nm), does indeed suggest that the primary photoacceptor for these two wavelengths (810 nm and 980 nm) may indeed be different. There have been a few clinical reports where two NIR wavelengths such as 810 nm and 980 nm have been combined together [28, 29]

Nevertheless, most authors (including ourselves) had previously assumed that different NIR wavelengths (almost anything between 780 nm and 1200 nm) used in PBM, were likely to operate via the same basic mechanism. The present data suggests that this assumption will have to be re-addressed.

We wanted to test the hypothesis that 980 nm was absorbed by water in ion channels (possible some kind of structured water that could form a selectively absorbing cluster on specific surface structures; this phenomenon has been called “near-surface water” by Pollack and colleagues [30]). The literature had already suggested that TRPV1 is a candidate ion channel that could be activated in PBM protocols [31–33]. Therefore we chose to use two different inhibitors of TRP ion channels (CPZ which is fairly specific for TRPV1 [34], and SKF which is less specific [35]). Both of these inhibitors blocked many of the effects of 980 nm, but had little to no blocking activity on the cellular effects of 810 nm PBM. Since we

hypothesized that 980 nm was acting by heating up microscopic regions of water in important locations within the cell (such as ion channels) we decided to test the effect of cold and heat on the cellular effects of PBM. The rationale for using cold (4°C during the PBM) was that very small, microscopic changes in the temperature of protein domains caused by absorption of 980 nm by near-surface water, would be “lost” when the bulk temperature was reduced. Likewise, we reasoned that if the temperature was raised to 42°C, the effect of these microscopic temperature gradients caused by water absorption of 980 nm would also be ineffective owing to the bulk temperature having been raised. The fact that both heat and cold treatments abrogated the effects of 980 nm laser, but not the effects of 810 nm suggests that heat-gated ion channels can be activated by 980 nm but not by 810 nm.

The possibility of water acting as a chromophore in PBM studies has previously been discussed by Santana-Blank [36, 37] and Sommer [38, 39] (among others). Further studies will be necessary to confirm or refute this hypothesis.

Previously we had carried out studies comparing PBM with four different wavelengths, 660, 730, 810, and 980 nm in a mouse model of healing of partial thickness abrasion wounds [40]. We delivered the same fluence from all four lasers (4 J/cm^2) at a constant irradiance (10 mW/cm^2). We found that 635 nm and 810 nm were significantly effective in promoting healing, but 730-nm and 980-nm wavelengths showed no improvement in healing. 810-nm gave the highest decrease in wound area ($p < 0.05$), enhanced collagen accumulation, and complete re-epithelialization as compared to other wavelengths and non-illuminated controls.

Moreover we also tested these same four wavelengths in a mouse model of closed head (weight drop) traumatic brain injury (TBI) [41]. We applied a single exposure of the closed mouse head to 36 J/cm2 delivered at 150 mW/cm2, 4 hours after the TBI injury was created. Again the overall results were somewhat similar, with the 660 nm and 810 nm wavelengths producing a significant improvement in neurological severity score that increased over the course of the follow-up compared to sham-treated controls., that was not seen with the 730 nm and 980 nm wavelengths.

How can we explain the fact, that in two separate studies we found 980 nm to be ineffective, while 810 was highly effective, while in the present study we find that 980 nm has positive effects in vitro? We believe the answer lies in the biphasic dose response observed for both 810 nm and 980 nm in the present study. The peak response to 980 nm in the SRB assay was found with 0.3 J/cm2, while with 810 nm the peak response was seen at 3 J/cm2. Therefore it appears that much lower fluences of 980 nm are required, compared to the fluences of 810 nm needed. It is likely that in the two studies referred to above (mouse wound healing and closed head TBI) we simply used too high a dose of 980 nm. If we had used a much lower dose (one tenth) we may well have found that 980 nm did in fact have a positive beneficial effect.

A group of investigators from Turkey published a series of three papers [42–44], all looking at the same animal model, in which rats were injected IP with 5-fluorouracil, and then had the inside of their cheek mucosa scratched with a needle to simulate oral mucositis. They

treated these rats with four different laser wavelengths, 660 nm, 810 nm, 980 nm and 1064 nm all with a dose of 8J/cm^2 delivered at different power densities. Overall the two longer wavelengths (980 nm and 1064 nm) gave more pronounced changes in expression of the different genes that were measured.

Anders and co-workers reported in 2014 that 980 nm light could inhibit the mitochondrial activity of human fibroblasts while 810 nm light at the same doses produced stimulation [25]. They also showed that much lower doses of 980 nm light were required to give the optimal stimulation of neurite elongation in cultured cortical neurons, than were needed for 810 nm light.

hASCs can be induced to differentiate to osteoblasts when cultured in OM using PBM, as reported by a number of investigators [14–16]. In agreement with these studies, we found that the optimum dose of 810 nm (3J/cm^2), and to a greater extent, the optimum dose of 980 nm (0.3J/cm^2) applied five times once every two days, increased AR staining and gene expression of RUNX2, OPN and OSX. When each of the 5 applications of PBM was preceded by a 10-min incubation with the ion channel inhibitors, CPZ and SKF, there was little difference in the osteogenic differentiation produced by 810 nm laser compared to that found without inhibitors. In contrast the osteogenic differentiation produced by 980 nm was substantially abrogated by the use of these pharmacological ion channel inhibitors.

It should be noted that our studies were entirely carried out with human ADSC. Stem cells, adipocytes and cells in general have differing responses to light and other cellular environmental perturbations. Heat and cold do alter the biology of adipocytes and have been discussed as potential means for converting white to beige fat as a way of managing obesity for example. It is also of note that timing between the PBM intervention and the heat or cold stress (before, during or after) is likely to play a role. Many complex stress response pathways have been described that are triggered by heat shock [45] and cold shock [46], and it will ne necessary to closely examine the effects of these pathways on the PBM response.

In conclusion, we have found evidence that the mechanisms of action of 810 nm and 980 nm laser appear to have significant differences. A reasonable hypothesis to explain the mechanism of action of 980 nm relies on the activation of heat (or light)-gated ion channels. However activation of CCO in mitochondria by 810 nm continues to be the most important and generally accepted mechanism. Our results raise a host of questions that will need to be answered by future studies. Do other cell types (in addition to the presently studied hASCs) behave in a similar manner? Do other wavelengths that are longer than 980 nm (for instance 1064 nm or 1260 nm) behave in a similar manner to 980 nm? Why should activation of heat-gated ion channels produce increases in ATP and MMP in the same manner as 810 nm. Why should activation of ion channels produce ROS? Will the much lower optimum fluences of 980 nm that are apparently needed in vitro, translate into greater clinical efficacy when this wavelength is used in vivo?

Acknowledgments

This work was supported by US NIH R01AI050875 and by Air Force Office of Scientific Research grant FA9550-13-1-0068, US Army Medical Research Acquisition Activity grant W81XWH-09-1-0514, and US Army

Medical Research and Materiel Command grant W81XWH-13-2-0067. Yuguang Wang was funded by PKUSS grant PKUSS20140208 and Ministry of Education grant 113002A.

References

1. Chung H, Dai T, Sharma SK, Huang YY, Carroll JD, Hamblin MR. The nuts and bolts of low-level laser (light) therapy. Ann Biomed Eng. 2012; 40:516–533. [PubMed: 22045511]
2. Anders JJ, Lanzafame RJ, Arany PR. Low-level light/laser therapy versus photobiomodulation therapy. Photomed Laser Surg. 2015; 33:183–184. [PubMed: 25844681]
3. De Freitas LF, Hamblin MR. Proposed Mechanisms of Photobiomodulation or Low-Level Light Therapy. IEEE Journal of Selected Topics in Quantum Electronics. 2016; 22:7000417.
4. Wong-Riley MT, Liang HL, Eells JT, Chance B, Henry MM, Buchmann E, Kane M, Whelan HT. Photobiomodulation directly benefits primary neurons functionally inactivated by toxins: role of cytochrome c oxidase. J Biol Chem. 2005; 280:4761–4771. [PubMed: 15557336]
5. Lane N. Cell biology: power games. Nature. 2006; 443:901–903. [PubMed: 17066004]
6. Vatansever F, Hamblin MR. Far infrared radiation (FIR): its biological effects and medical applications. Photonics Lasers Med. 2012; 4:255–266. [PubMed: 23833705]
7. Lavi R, Ankri R, Sinyakov M, Eichler M, Friedmann H, Shainberg A, Breitbart H, Lubart R. The plasma membrane is involved in the visible light-tissue interaction. Photomed Laser Surg. 2012; 30:14–19. [PubMed: 21967485]
8. Barboza CA, Ginani F, Soares DM, Henriques AC, Freitas Rde A. Low-level laser irradiation induces in vitro proliferation of mesenchymal stem cells. Einstein (Sao Paulo). 2014; 12:75–81. [PubMed: 24728250]
9. Bouvet-Gerbettaz S, Merigo E, Rocca JP, Carle GF, Rochet N. Effects of low-level laser therapy on proliferation and differentiation of murine bone marrow cells into osteoblasts and osteoclasts. Lasers Surg Med. 2009; 41:291–297. [PubMed: 19347941]
10. de Villiers JA, Houreld NN, Abrahamse H. Influence of low intensity laser irradiation on isolated human adipose derived stem cells over 72 hours and their differentiation potential into smooth muscle cells using retinoic acid. Stem Cell Rev. 2011; 7:869–882. [PubMed: 21373882]
11. Eduardo Fde P, Bueno DF, de Freitas PM, Marques MM, Passos-Bueno MR, Eduardo Cde P, Zatz M. Stem cell proliferation under low intensity laser irradiation: a preliminary study. Lasers Surg Med. 2008; 40:433–438. [PubMed: 18649378]
12. Kushibiki T, Hirasawa T, Okawa S, Ishihara M. Low Reactive Level Laser Therapy for Mesenchymal Stromal Cells Therapies. Stem Cells Int. 2015; 2015:974864. [PubMed: 26273309]
13. Park IS, Chung PS, Ahn JC. Enhanced angiogenic effect of adipose-derived stromal cell spheroid with low-level light therapy in hind limb ischemia mice. Biomaterials. 2014; 35:9280–9289. [PubMed: 25132605]
14. Abramovitch-Gottlib L, Gross T, Naveh D, Geresh S, Rosenwaks S, Bar I, Vago R. Low level laser irradiation stimulates osteogenic phenotype of mesenchymal stem cells seeded on a three-dimensional biomatrix. Lasers Med Sci. 2005; 20:138–146. [PubMed: 16292614]
15. Choi K, Kang BJ, Kim H, Lee S, Bae S, Kweon OK, Kim WH. Low-level laser therapy promotes the osteogenic potential of adipose-derived mesenchymal stem cells seeded on an acellular dermal matrix. J Biomed Mater Res B Appl Biomater. 2013; 101:919–928. [PubMed: 23529895]
16. Peng F, Wu H, Zheng Y, Xu X, Yu J. The effect of noncoherent red light irradiation on proliferation and osteogenic differentiation of bone marrow mesenchymal stem cells. Lasers Med Sci. 2012; 27:645–653. [PubMed: 22016038]
17. Vichai V, Kirtikara K. Sulforhodamine B colorimetric assay for cytotoxicity screening. Nat Protoc. 2006; 1:1112–1116. [PubMed: 17406391]
18. Romanovsky AA, Almeida MC, Garami A, Steiner AA, Norman MH, Morrison SF, Nakamura K, Burmeister JJ, Nucci TB. The transient receptor potential vanilloid-1 channel in thermoregulation: a thermosensor it is not. Pharmacol Rev. 2009; 61:228–261. [PubMed: 19749171]
19. Choudhery MS, Badowski M, Muise A, Harris DT. Effect of mild heat stress on the proliferative and differentiative ability of human mesenchymal stromal cells. Cytotherapy. 2015; 17:359–368. [PubMed: 25536863]

20. Ytteborg E, Vegusdal A, Witten PE, Berge GM, Takle H, Ostbye TK, Ruyter B. Atlantic salmon (Salmo salar) muscle precursor cells differentiate into osteoblasts in vitro: polyunsaturated fatty acids and hyperthermia influence gene expression and differentiation. Biochim Biophys Acta. 2010; 1801:127–137. [PubMed: 19833228]
21. Skopin MD, Molitor SC. Effects of near-infrared laser exposure in a cellular model of wound healing. Photodermatol Photoimmunol Photomed. 2009; 25:75–80. [PubMed: 19292782]
22. Cafaro A, Arduino PG, Massolini G, Romagnoli E, Broccoletti R. Clinical evaluation of the efficiency of low-level laser therapy for oral lichen planus: a prospective case series. Lasers Med Sci. 2014; 29:185–190. [PubMed: 23549680]
23. Dukic W, Bago I, Aurer A, Roguljic M. Clinical effectiveness of diode laser therapy as an adjunct to non-surgical periodontal treatment: a randomized clinical study. J Periodontol. 2013; 84:1111–1117. [PubMed: 23075433]
24. Ferrante M, Petrini M, Trentini P, Perfetti G, Spoto G. Effect of low-level laser therapy after extraction of impacted lower third molars. Lasers Med Sci. 2013; 28:845–849. [PubMed: 22843310]
25. Anders JJ, Moges H, Wu X, Erbele ID, Alberico SL, Saidu EK, Smith JT, Pryor BA. In vitro and in vivo optimization of infrared laser treatment for injured peripheral nerves. Lasers Surg Med. 2014; 46:34–45. [PubMed: 24338500]
26. Plapler H, Mancini MW, Sella VR, Bomfim FR. Evaluation of different laser wavelengths on ablation lesion and residual thermal injury in intervertebral discs of the lumbar spine. Lasers Med Sci. 2016; 31:421–428. [PubMed: 26796705]
27. Sydnor M, Mavropoulos J, Slobodnik N, Wolfe L, Strife B, Komorowski D. A randomized prospective long-term (>1 year) clinical trial comparing the efficacy and safety of radiofrequency ablation to 980 nm laser ablation of the great saphenous vein. Phlebology. 2016
28. Henderson TA, Morries LD. SPECT Perfusion Imaging Demonstrates Improvement of Traumatic Brain Injury With Transcranial Near-infrared Laser Phototherapy. Adv Mind Body Med. 2015; 29:27–33.
29. Slot DE, Jorritsma KH, Cobb CM, Van der Weijden FA. The effect of the thermal diode laser (wavelength 808–980 nm) in non-surgical periodontal therapy: a systematic review and meta-analysis. J Clin Periodontol. 2014; 41:681–692. [PubMed: 24460795]
30. Chai B, Yoo H, Pollack GH. Effect of radiant energy on near-surface water. J Phys Chem B. 2009; 113:13953–13958. [PubMed: 19827846]
31. Gu Q, Wang L, Huang F, Schwarz W. Stimulation of TRPV1 by Green Laser Light. Evid Based Complement Alternat Med. 2012; 2012:857123. [PubMed: 23365602]
32. Wang L, Zhang D, Schwarz W. TRPV Channels in Mast Cells as a Target for Low-Level-Laser Therapy. Cells. 2014; 3:662–673. [PubMed: 24971848]
33. Wu ZH, Zhou Y, Chen JY, Zhou LW. Mitochondrial signaling for histamine releases in laser-irradiated RBL-2H3 mast cells. Lasers Surg Med. 2010; 42:503–509. [PubMed: 20662027]
34. Pal M, Angaru S, Kodimuthali A, Dhingra N. Vanilloid receptor antagonists: emerging class of novel anti-inflammatory agents for pain management. Curr Pharm Des. 2009; 15:1008–1026. [PubMed: 19275664]
35. Ding J, Zhang JR, Wang Y, Li CL, Lu D, Guan SM, Chen J. Effects of a non-selective TRPC channel blocker, SKF-96365, on melittin-induced spontaneous persistent nociception and inflammatory pain hypersensitivity. Neurosci Bull. 2012; 28:173–181. [PubMed: 22466128]
36. Santana-Blank L, Rodriguez-Santana E, Santana-Rodriguez K. Theoretic, experimental, clinical bases of the water oscillator hypothesis in near-infrared photobiomodulation. Photomed Laser Surg. 2010; 28(Suppl 1):S41–52. [PubMed: 20649429]
37. Santana-Blank LA, Rodriguez-Santana E, Santana-Rodriguez KE. Photo-infrared pulsed bio-modulation (PIPBM): a novel mechanism for the enhancement of physiologically reparative responses. Photomed Laser Surg. 2005; 23:416–424. [PubMed: 16144487]
38. Sommer AP. A mechanism for ultrasound/light-induced biostimulation. Ann Transl Med. 2015; 3:291. [PubMed: 26697451]
39. Sommer AP, Haddad M, Fecht HJ. Light Effect on Water Viscosity: Implication for ATP Biosynthesis. Sci Rep. 2015; 5:12029. [PubMed: 26154113]

40. Gupta A, Dai T, Hamblin MR. Effect of red and near-infrared wavelengths on low-level laser (light) therapy-induced healing of partial-thickness dermal abrasion in mice. Lasers Med Sci. 2013

41. Wu Q, Xuan W, Ando T, Xu T, Huang L, Huang YY, Dai T, Dhital S, Sharma SK, Whalen MJ, Hamblin MR. Low-level laser therapy for closed-head traumatic brain injury in mice: effect of different wavelengths. Lasers Surg Med. 2012; 44:218–226. [PubMed: 22275301]

42. Bostancikliogl u M, Demiryurek S, Cengiz B, Demir T, Oztuzcu S, Aras MH, Ozsevik S, Usumez A, Ergun S, Ozbal HK, Bagci C. Assessment of the effect of laser irradiations at different wavelengths (660, 810, 980, and 1064 nm) on autophagy in a rat model of mucositis. Lasers Med Sci. 2015; 30:1289–1295. [PubMed: 25732242]

43. Isman E, Aras MH, Cengiz B, Bayraktar R, Yolcu U, Topcuoglu T, Usumez A, Demir T. Effects of laser irradiation at different wavelengths (660, 810, 980, and 1064 nm) on transient receptor potential melastatin channels in an animal model of wound healing. Lasers Med Sci. 2015; 30:1489–1495. [PubMed: 25863514]

44. Usumez A, Cengiz B, Oztuzcu S, Demir T, Aras MH, Gutknecht N. Effects of laser irradiation at different wavelengths (660, 810, 980, and 1,064 nm) on mucositis in an animal model of wound healing. Lasers Med Sci. 2014; 29:1807–1813. [PubMed: 23636299]

45. Morimoto RI. The heat shock response: systems biology of proteotoxic stress in aging and disease. Cold Spring Harb Symp Quant Biol. 2011; 76:91–99. [PubMed: 22371371]

46. Saita E, Albanesi D, de Mendoza D. Sensing membrane thickness: Lessons learned from cold stress. Biochim Biophys Acta. 2016; 1861:837–846. [PubMed: 26776056]

Highlights

- Photobiomodulation was tested in adipose-derived stem cells (ADSC)
- Both 810nm and 980nm showed a biphasic dose response for proliferation and ATP
- Optimum dose (J/cm^2) was 10–10 times lower for 980 nm than for 810nm
- Effects of 980nm (but not 810nm) could be abrogated by ion-channel inhibitors
- Effects of 980nm (but not 810nm) could be abrogated by heat and cold treatment
- 980nm-mediated differentiation of ADSC into osteoblasts could be abrogated as above.

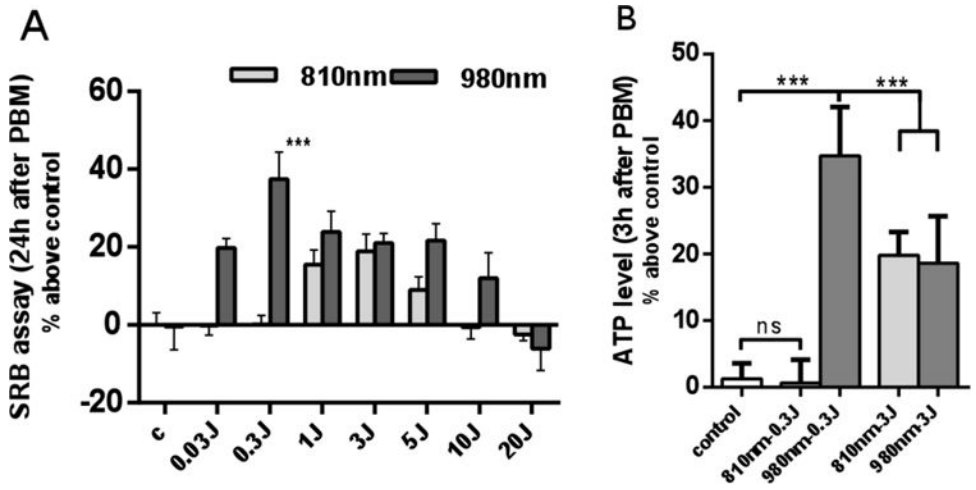

Figure 1. Biphasic dose response of 810 nm and 980 nm

(A) Quantitative analysis of cell proliferation 24 hours after 810nm and 980nm PBM by SRB assay. Data represent mean ± SEM. (B) Quantitative analysis of ATP production level 3 hours after PBM. (n=8; $^{***}P<0.001$)

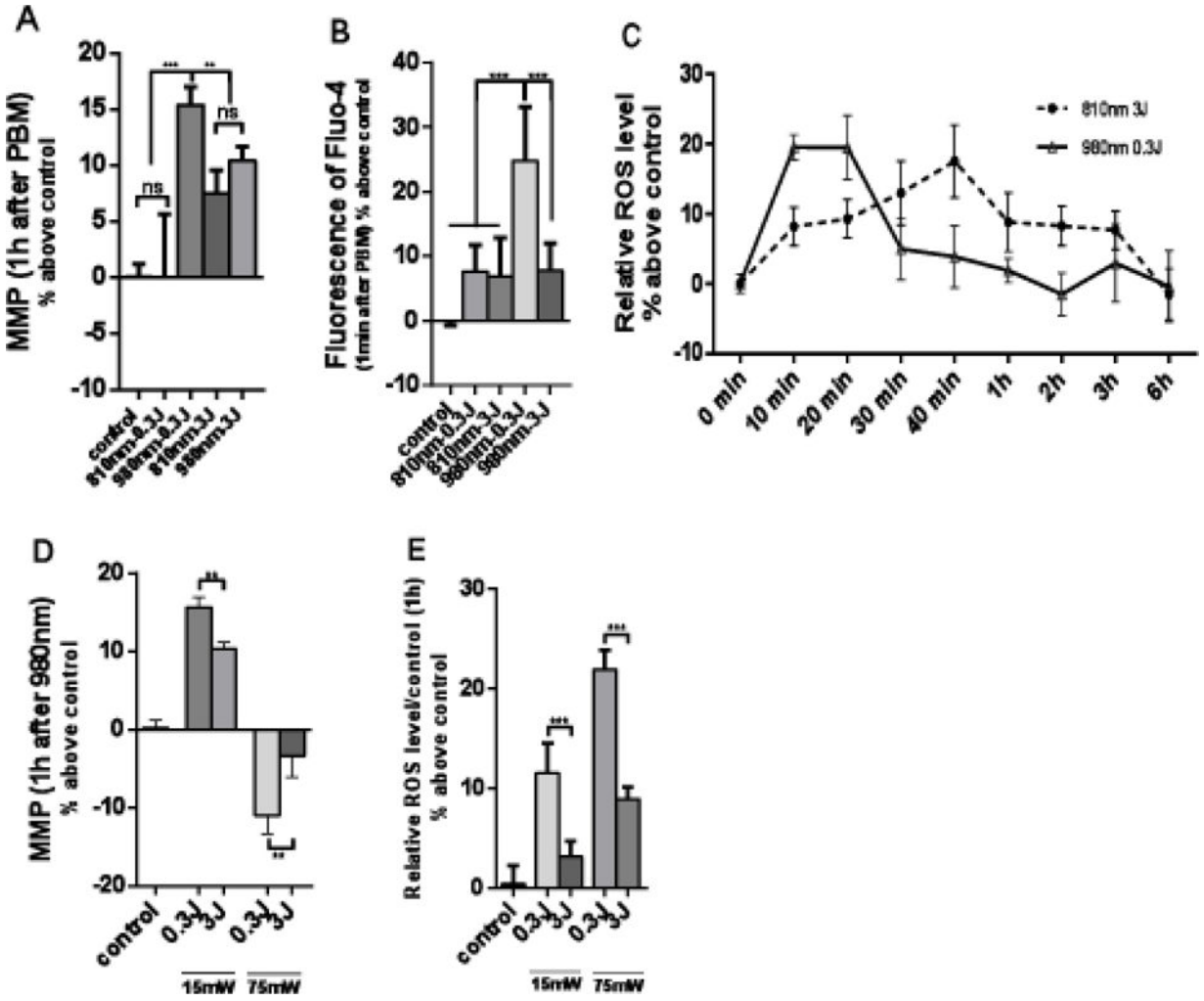

Figure 2. Effects of 810 nm and 980 nm on MMP, intracellular calcium, and ROS production at different fluences and power densities

(A) MMP measured 1 hour after photobiomodulation. (B) Intracellular calcium measured within 1 minute after photobiomodulation. (C) Time course of ROS production. (D) MMP 1 hour after photobiomodulation, comparing 15mW/cm^2, 75mW/cm^2 of 980 nm at doses of 0.3 J/cm^2 and 3 J/cm^2. (E) ROS 1 hour after photobiomodulation, comparing 15mW/cm^2, 75mW/cm^2 of 980 nm at doses of 0.3 J/cm^2 and 3 J/cm^2. Data represent mean ± SEM. All data are expressed as percentage above control. (n=6 or 8; **P<0.01, ***P<0.001)

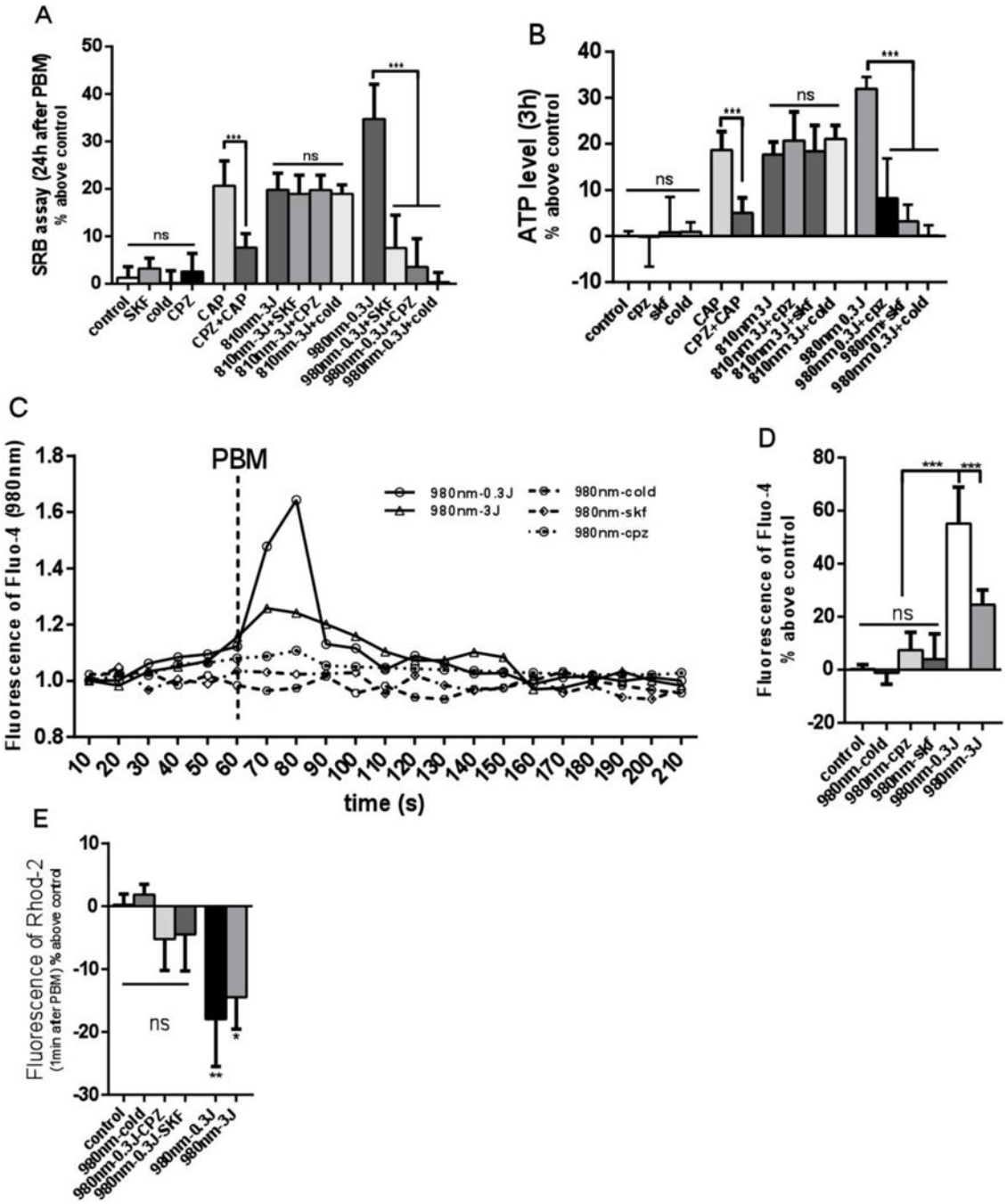

Figure 3. Effects of 980 nm photobiomodulation on cytosolic and mitochondrial calcium could be abrogated by CPZ, SKF and cold treatment

(A) Cell proliferation. (B) ATP production. (C) Time course of intracellular calcium, PBM was used at 60s, a peak was found within 30 seconds. (D) Intracellular calcium 30 seconds after PBM. (E) Mitochondrial calcium 30 seconds after PBM. Data represent mean ± SEM. (n=6 or 8; $^{*}P<0.05$, $^{**}P<0.01$, $^{***}P<0.001$)

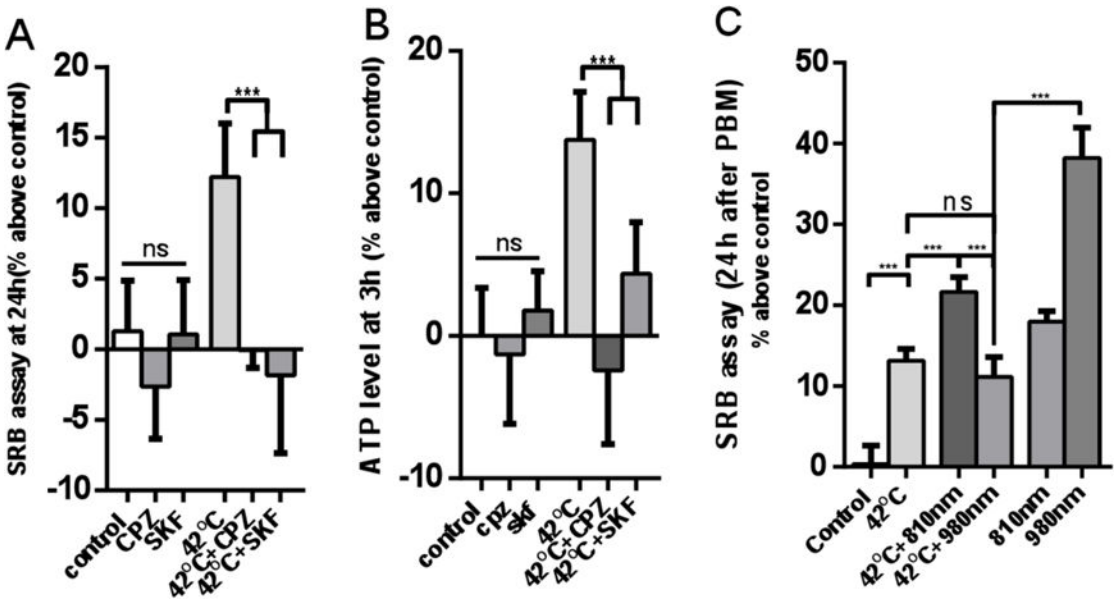

Figure 4. The effect of heat treatment, TRP inhibitors, and combination of heat and PBM (0.3 J/cm^2 of 980 nm and 3 J/cm^2 of 810 nm) on cell proliferation and ATP

(A) Cell proliferation with or without TPRV1 inhibitor before heat treatment. (B) ATP production with or without TPRV1 inhibitor before heat treatment. (C) Cell proliferation after combination of heat and PBM. Data represent mean ± SEM. (n=6 or 8; ***P<0.001).

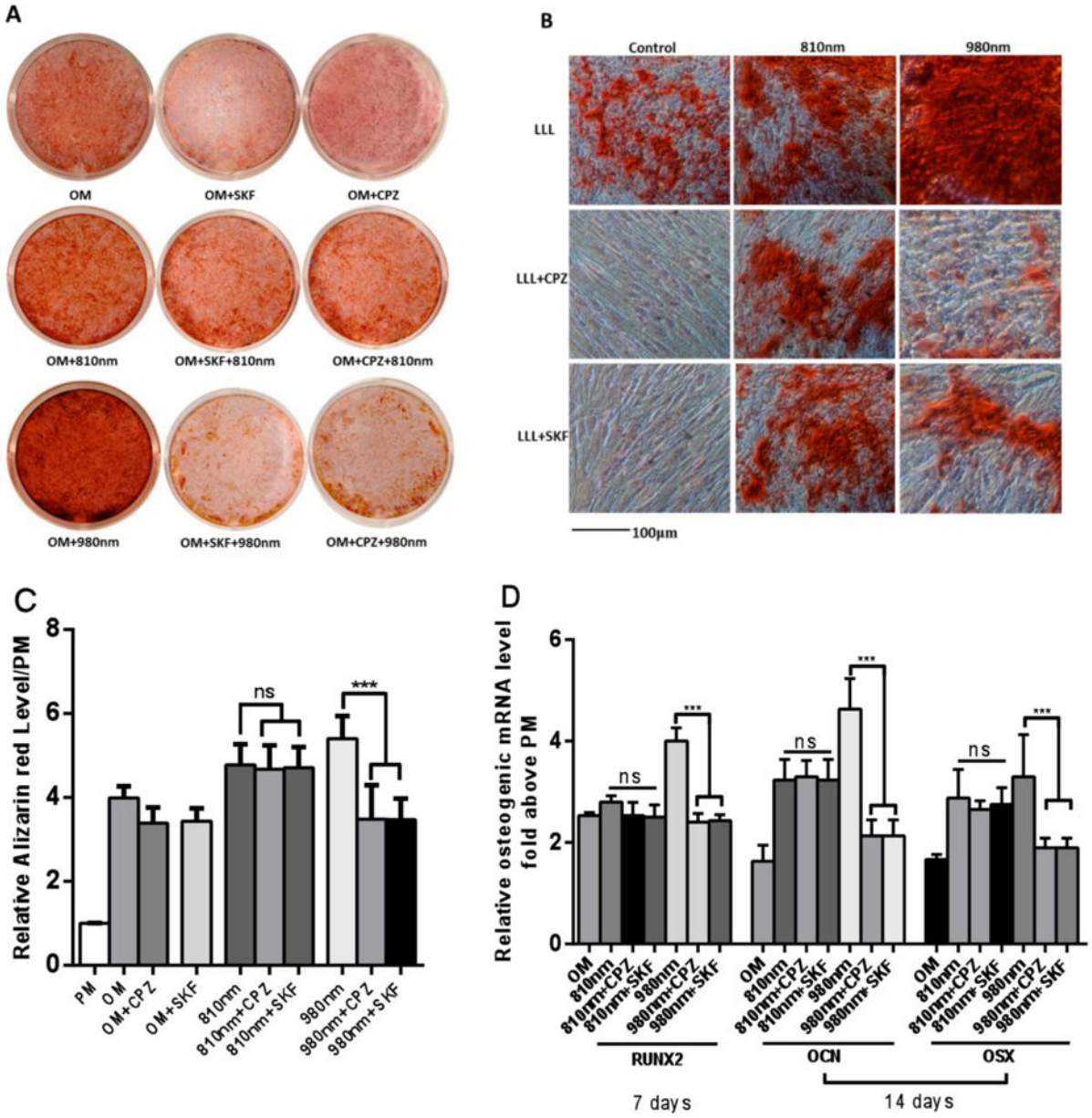

Figure 5. Effects of 810 nm and 980 nm PBM on hASCS differentiation

A. Macroscopic view of Alizarin Red staining after 810 nm and 980 nm PBM on day 21. B. Microscopic view of Alizarin red staining (scale bar 100 μm). C. Quantitative detection of Alizarin Red staining after 810 nm and 980 nm PBM. D. Quantitative detection of the expression level of osteogenic-related genes using RT-PCR after 810 nm and 980 nm PBM. Data represent mean ± SEM. (n=6 or 8; $^{***}P<0.001$)

Table 1

Light sources and parameters

Wavelength	**810 nm**		**980 nm**	
Type	Diode laser		Diode laser	
Manufacture	Opto Power Corp., Tucson, AZ, USA		B&W TEK, Newark, DE, USA	
Models	Model D030-MM-FCTS/B		POLAR-980-10	
Mode	CW		CW	
Total power (W)	1	1	1	1
Irradiance (mW/cm^2)	16	16	16	16
Fluence (J/cm^2)	3	0.3	3	0.3
Time of irradiation (S)	188	18.8	188	18.8
Spot size (cm^2)	4	4	4	4

The irradiance was adjusted by changing the distance between the laser and the cell culture dish. The cell culture plates were covered with aluminum-foil, the spot size was defined by the size of window in the aluminum-foil. CW = continuous-wave.

Table 2

The primers for qPCR Analysis

	Forward primer	Reverse primer
ALP	ATGGGATGGGTGTCTCCACA	CCACGAAGGGGAACTTGTC
RUNX2	CCGCCTCAGTGATTTAGGGC	GGGTCTGTAATCTGACTCTGTCC
OCN	CACTCCTCGCCCTATTGGC	CCCTCCTGCTTGGACACAAAG
OSX	AGCAGCAGTAGCAGAAGCA	CAGCAGTCCCATAGGCATC
GAPDH	GGTCACCAGGGCTGCTTTTA	GGATCTCGCTCCTGGAAGATG
TRPV1	GATGGCAAGGACGACTACCG	TGTCTGCCTGAAACTCTGCTTG
TRPV2	CGCACCGACACCGAATG	ATGGTAGGCAACAGCGGTG
TRPV3	CCATCCAATCCCAACAGCC	ACTCTACCAACTCCTCCACGC
TRPV4	GCCGTGATGGTCTTTGCC	AGACGAGCAGGAATCGGAAA
TRPV5	GTGGCAACCGCACTCATTC	GAGAGGCACCAACCCTGAAG
TRPV6	CACCTTCGAGCTGTTCCTTACC	CCAGTGAGTGTCGCCCATC